

## Harmonic Analysis of A Random Zero Vector Distribution Space Vector Pulse Width Modulation

Guoqiang Chen and Jianli Kang

*School of Mechanical and Power Engineering, Henan Polytechnic University,  
Jiaozuo, 454000, China  
jz97cgq@sina.com*

### **Abstract**

*Aiming at complicated characteristic analysis and implementation of the randomization space vector pulse width modulation (SVPWM) scheme, a new random zero-vector SVPWM scheme with a fixed randomization range is proposed. The fixed range is a linear function of the modulation index. Firstly, the principle of the new scheme is given. In addition, the implicit modulating voltages, the derivation procedure of the micro and macro harmonic distortion factor (HDF) are presented in detail, and the Monte Carlo method is proposed to efficiently analyze the HDF. Finally, the harmonic spectrum of the new scheme is analyzed compared with the commonly used symmetrical 7-segment SVPWM scheme through an example, and the result verifies its excellent performance on suppressing the cluster harmonic magnitude around the integer multiple switching frequency.*

**Keywords:** *Space vector pulse width modulation, Random zero-vector distribution, Harmonic distortion factor, Random variable*

### **1. Introduction**

Pulse width modulation (PWM) has been widely used in all kinds of fields that require the power conversion, for example, between the alternating current (AC) power source and the direct current (DC) source. The space vector PWM (SVPWM) strategy is one of the key modulation strategies to control the two-level three-phase inverter. Because SVPWM is based on the volt-second balance principle, the harmonic is inevitable besides the required fundamental or first harmonic [1-4]. The harmonic has serious effects on performance of the application, such as the losses in the load motor [2], the dynamic operational characteristics of the closed-loop system [5], EMI (Electromagnetic Interference)[6] and audible noise [7]. The SVPWM strategy can be classified into the deterministic strategy and the random strategy. The deterministic strategy presents cluster harmonics with large magnitudes around the multiples of the switching frequency, especially for the fixed switching frequency SVPWM strategy. In order to suppress the peak harmonics and reduce the serious undesirable effects, randomization has been used to spread the harmonics continuously to a wideband area, so the cluster peak harmonics can be reduced greatly [8-14]. Almost every parameter in SVPWM can be randomized in theory, so there are lots of randomization or chaos schemes. The most intuitional randomization scheme includes random zero-vector distribution SVPWM (RZDSVPWM), random switching frequency SVPWM (RSFSVPWM) and random pulse position SVPWM (RPPSVPWM). Hybrid SVPWM (HSVPWM) includes more than two randomization factors, such as the zero-vector distribution ratio, the switching frequency and the pulse position. Characteristic analysis and implementation of the randomization SVPWM scheme is always complicated, so too many randomization schemes have not been used in reality until now. Although the implementation problem can be solved with the development of the micro controller unit chips in the future, the new randomization

SVPWM scheme is therefore needed of which the scheme can be easily implemented in the up-to-date control unit and the characteristic can be easily analyzed[15]. In this paper, a new RZDSVPWM scheme is proposed and harmonic characteristic is presented and discussed.

## 2. Principle of SVPWM

The topology of the classic three-phase two-level inverter is shown in Figure 1[1-4]. The DC link voltage is  $U_{DC}$ . The inverter gives two voltage levels (0 and  $U_{DC}$ ) with respect to the negative rail N or ( $-U_{DC}/2$  and  $U_{DC}/2$ ) with respect to the neutral point O. The inverter has 8 permissible states that are corresponding to the 8 basic space vectors as shown in Figure 2. An arbitrary command/reference voltage vector  $\vec{u}_s$  with the vector amplitude  $u_s$  and the phase angle  $\theta$  inside the hexagon region shown in Figure 2 can be generated by two adjacent active vectors (for example  $\vec{u}_1$  and  $\vec{u}_2$  in the first sextant) and the zero vectors. The on-state duration time  $t_1$ ,  $t_2$  and  $t_0$  of the three vectors are determined by the identical volt-second balance at the periodical time interval  $T_s$  using Equation (1). There are large numbers of vector operation modes that satisfy this equation.

$$T_s \vec{u}_s = T_1 \vec{u}_1 + T_2 \vec{u}_2 \quad (1)$$

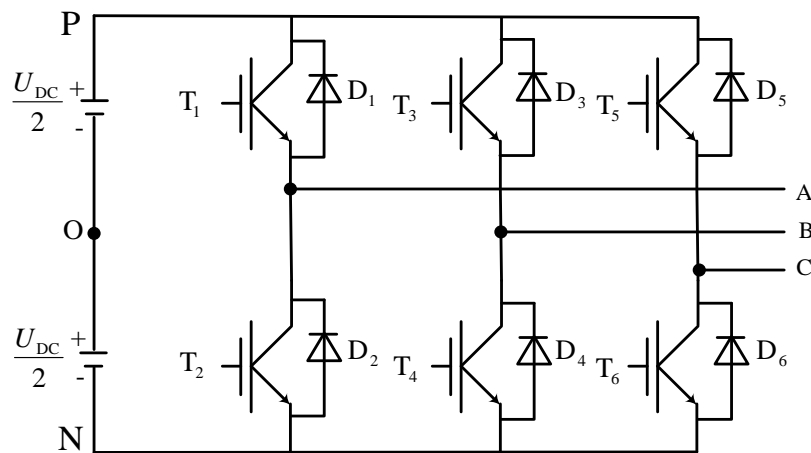


**Figure 1. The Topology of the Two-Level Three-Phase Inverter**  
 The notations P, O and N Refer to That the Three Phase Output Terminals are Positive, Zero and Negative, Respectively

For the commonly used 7-segment SVPWM scheme operation of the inverter, the switching pulse waveforms for the upper arms in the 6 sextants are shown in Figure 2. The vector sequences in the 6 sextants are

$$\begin{cases} \vec{U}_0(000) \rightarrow \vec{U}_1(100) \rightarrow \vec{U}_2(110) \rightarrow \vec{U}_7(111) \rightarrow \vec{U}_2(110) \rightarrow \vec{U}_1(100) \rightarrow \vec{U}_0(000) & \text{I} \\ \vec{U}_0(000) \rightarrow \vec{U}_3(100) \rightarrow \vec{U}_2(110) \rightarrow \vec{U}_7(111) \rightarrow \vec{U}_2(110) \rightarrow \vec{U}_3(100) \rightarrow \vec{U}_0(000) & \text{II} \\ \vec{U}_0(000) \rightarrow \vec{U}_3(100) \rightarrow \vec{U}_4(110) \rightarrow \vec{U}_7(111) \rightarrow \vec{U}_4(110) \rightarrow \vec{U}_3(100) \rightarrow \vec{U}_0(000) & \text{III} \\ \vec{U}_0(000) \rightarrow \vec{U}_5(100) \rightarrow \vec{U}_4(110) \rightarrow \vec{U}_7(111) \rightarrow \vec{U}_4(110) \rightarrow \vec{U}_5(100) \rightarrow \vec{U}_0(000) & \text{IV} \\ \vec{U}_0(000) \rightarrow \vec{U}_5(100) \rightarrow \vec{U}_6(110) \rightarrow \vec{U}_7(111) \rightarrow \vec{U}_6(110) \rightarrow \vec{U}_5(100) \rightarrow \vec{U}_0(000) & \text{V} \\ \vec{U}_0(000) \rightarrow \vec{U}_1(100) \rightarrow \vec{U}_6(110) \rightarrow \vec{U}_7(111) \rightarrow \vec{U}_6(110) \rightarrow \vec{U}_1(100) \rightarrow \vec{U}_0(000) & \text{VI} \end{cases} \quad (2)$$

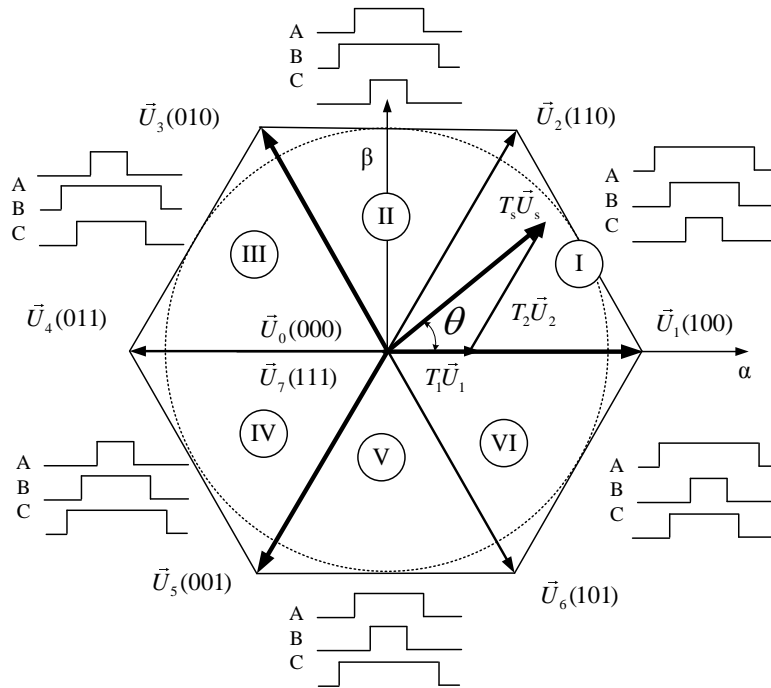


**Figure 2. The Vector Diagram and the Vector Summation Method. The Pulse Waveforms Following the Notations A, B and C Refer to the Upper Arm Control Signals for the Three Phases.  $\vec{U}_0(000)$ ,  $\vec{U}_1(100)$ ,  $\vec{U}_2(110)$ ,  $\vec{U}_3(010)$ ,  $\vec{U}_4(011)$ ,  $\vec{U}_5(001)$ ,  $\vec{U}_6(101)$  and  $\vec{U}_7(111)$  Refer to the 8 Basic Voltage Vectors**

### 3. New RZDSVPWM Scheme

The duration time for the two basic active space vectors in the first sextant is

$$\begin{cases} T_1 = \frac{\sqrt{3}}{2} M T_s \sin(\pi/3 - \theta) \\ T_2 = \frac{\sqrt{3}}{2} M T_s \sin \theta \end{cases} \quad (3)$$

where  $\theta$  is the phase angle of the command/reference voltage vector,  $T_s$  is the switching period, and  $M$  is the modulation index corresponding to the command/reference voltage vector.

With the vector amplitude  $U_o$ , the modulation index  $M$  is always given by

$$M = \frac{U_o}{U_{DC}/2} \quad (4)$$

The total duration time of the two zero vectors ( $T_{00}$  for  $\vec{U}_0$  and  $T_{07}$  for  $\vec{U}_7$ ) is

$$\begin{aligned} T_0 &= T_s - T_1 - T_2 = T_{00} + T_{07} \\ &= T_s \left( 1 - \frac{\sqrt{3}}{2} M \sin(\pi/3 + \theta) \right) \quad (0 \leq \theta \leq \pi/3) \end{aligned} \quad (5)$$

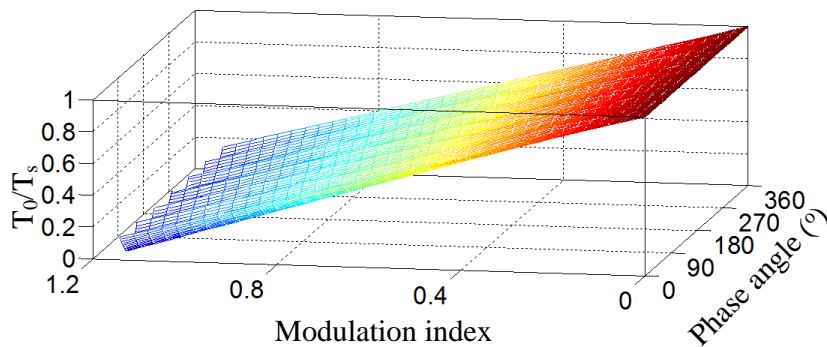
When  $\theta = \pi/6$  the duration time reaches the minimum value

$$T_{0\min} = T_s \left( 1 - \frac{\sqrt{3}}{2} M \right) \quad (6)$$

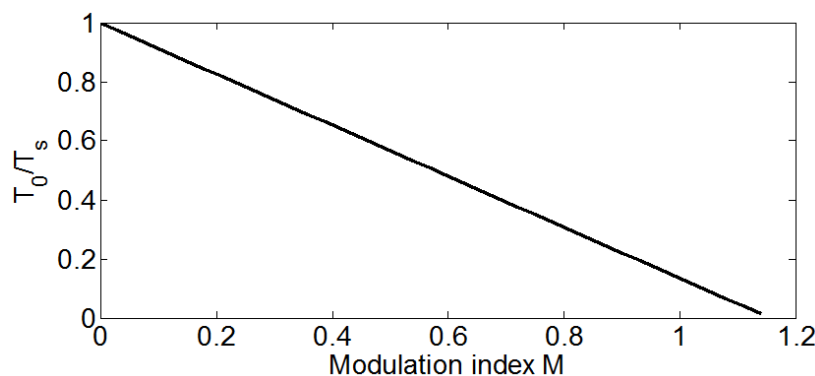
The randomization range of the zero-vectors  $\vec{u}_0$  and  $\vec{u}_7$  is set as  $T_{0\min}$ . If the zero vector duration time distribution ratio is  $R$ , the duration time  $T_{00}$  for  $\vec{u}_0$  and  $T_{07}$  for  $\vec{u}_7$  is

$$\begin{cases} T_{00} = RT_{0\min} + \frac{1}{2}(T_0 - T_{0\min}) \\ T_{07} = (1 - R)T_{0\min} + \frac{1}{2}(T_0 - T_{0\min}) \end{cases} \quad (0 \leq R \leq 1) \quad (7)$$

The duration time of the zero vectors and the randomization range is shown in Figure 3. The duration time of the zero vectors is periodic with the period  $T_s/6$ , which is consistent with each sextant in Figure 2. It can be found that the total duration time of the two zero vectors reaches the minimum values at the center of each sextant, as shown in Figure 3(a). The total duration time increases with the decreasing of the modulation index. In the traditional RZDSVPWM scheme, all the total duration time of the zero vectors is randomized, so the randomization range changes with the phase angle. As shown in Figure 3(b), only a part of the total duration time is randomized and the randomization range is a linear function of the modulation index.



(a) The Duration Time of the Zero Vectors of the Deterministic SVPWM



(b) The Randomization Range of the New RZDSVPWM

**Figure 3. The Duration Time of The Zero Vectors and the Randomization Range**

## 4. Harmonic Distortion Factor

### 4.1. Theoretical Derivation

The harmonic distortion factor (HDF) is an important figure of the harmonic distortion and the micro HDF is defined as[2]

$$f(M, \theta) = \frac{\frac{1}{T_s} \int_0^{T_s} (\Delta i_{AB}^2 + \Delta i_{AC}^2 + \Delta i_{BC}^2) dt}{3 \left( \frac{U_{DC}}{2L_\sigma} \right)^2 \frac{T_s^2}{48}} \quad (8)$$

where  $L_\sigma$  is the equivalent line-line inductance for the delta connection with a prominent inductance load, and  $\Delta i_{AB}, \Delta i_{AC}, \Delta i_{BC}$  are the current ripples of line AB, AC and BC, respectively.

The macro HDF is defined as

$$F(M) = \frac{1}{2\pi} \int_0^{2\pi} f(M, \theta) d\theta \quad (9)$$

According to the result given by D.G. Holmes and T. A. Lipo [2], the average squared value of the current ripple of the line voltage over the switching interval/period is

$$\langle \Delta i_{12}^2 \rangle = \left( \frac{U_{DC}}{2L_\sigma} \right)^2 \frac{T_s^2}{48} \{ (u_2 - u_1)^2 + (u_2 - u_1)^3 + (u_2 - u_1)(u_2^3 - u_1^3) \} \quad (10)$$

where  $u_1$  and  $u_2$  are the per-unit voltages of two phases with the defined base unit quantity  $U_{DC}/2$ , and  $u_1 \geq u_2$ .

For example,

$$\begin{cases} u_1 = U_A / (U_{DC}/2) \\ u_2 = U_B / (U_{DC}/2) \end{cases} \quad (11)$$

where  $U_A$  and  $U_B$  are the phase leg references/implicit modulating voltages for Phase A and Phase B shown in Figure 1.

In the traditional SVPWM scheme the duration time in Equation (2) is symmetrical with respect to the midpoint of the switching period. From Figure 2, the reference average values of the three-phase voltages in the first sextant, expressed in terms of the neutral point O of the DC link, are

$$\begin{cases} U_A = \frac{U_{DC}}{2T_s} [(T_1 + T_2) + (T_{07} - T_{00})] = \frac{U_{DC}}{2T_s} (T_1 + T_2) + \frac{U_{DC}}{2T_s} (1 - 2R) T_{00} \\ U_B = \frac{U_{DC}}{2T_s} [(-T_1 + T_2) + (T_{07} - T_{00})] = \frac{U_{DC}}{2T_s} (-T_1 + T_2) + \frac{U_{DC}}{2T_s} (1 - 2R) T_{00} \\ U_C = \frac{U_{DC}}{2T_s} [(-T_1 - T_2) + (T_{07} - T_{00})] = \frac{U_{DC}}{2T_s} (-T_1 - T_2) + \frac{U_{DC}}{2T_s} (1 - 2R) T_{00} \end{cases} \quad (12)$$

The per-unit voltages of three phases with the base unit quantity  $U_{DC}/2$  can be expressed as

$$\begin{cases} u_A = \frac{U_A}{U_{DC}/2} = \frac{\sqrt{3}}{2} M \cos\left(\theta - \frac{\pi}{6}\right) + K \\ u_B = \frac{U_B}{U_{DC}/2} = \frac{3}{2} M \cos\left(\theta - \frac{2\pi}{3}\right) + K \\ u_C = \frac{U_C}{U_{DC}/2} = \frac{\sqrt{3}}{2} M \cos\left(\theta + \frac{5\pi}{6}\right) + K \end{cases} \quad (13)$$

where

$$K = \frac{1}{T_s}(1 - 2R)T_{00} = (1 - 2R)\left(1 - \frac{\sqrt{3}}{2}M\right).$$

Using Equations (8), (10) and (13) the micro HDF of the new RZDSVPWM can be computed with complex derivation as follows.

$$\begin{aligned} f(M, \theta) = & \frac{M^4}{32} \left( \begin{array}{l} -9 \cos 4\theta + 72\sqrt{3}R \cos 3\theta - 36\sqrt{3} \cos 3\theta - 18 \cos 2\theta \\ -72\sqrt{3}R \cos \theta + 36\sqrt{3} \cos \theta + 9\sqrt{3} \sin 4\theta - 18\sqrt{3} \sin 2\theta \\ + 216R \sin \theta - 108 \sin \theta + 432R^2 - 432R + 162 \end{array} \right) + \\ & + \frac{M^3}{4} \left( \begin{array}{l} -18R \cos 3\theta + 9 \cos 3\theta + 18R \cos \theta - 18 \cos \theta + \sqrt{3} \sin 3\theta \\ -18\sqrt{3}R \sin \theta + 6\sqrt{3} \sin \theta - 72\sqrt{3}R^2 + 72\sqrt{3}R - 18\sqrt{3} \end{array} \right) \\ & + (18R^2 - 18R + 6)M^2 \end{aligned} \quad (14)$$

Using Equations (9) and (14) the macro HDF can be computed in the first sextant as follows.

$$\begin{aligned} F(M) = & \frac{1}{\pi/3} \int_0^{\pi/3} f(M, \theta) d\theta \\ = & \frac{27}{2} \left( R^2 - R - \frac{3\sqrt{3}}{32} + \frac{3}{8} \right) M^4 + \left( -18\sqrt{3}R^2 + 18\sqrt{3}R - \frac{9\sqrt{3}}{2} - \frac{4\sqrt{3}}{\pi} \right) M^3 \\ & + (18R^2 - 18R + 6)M^2 \end{aligned} \quad (15)$$

The macro HDF can also be expressed as

$$\begin{aligned} F(M) = & \left( \frac{27}{2}M^4 - 18\sqrt{3}M^3 + 18M^2 \right) R^2 - \left( \frac{27}{2}M^4 - 18\sqrt{3}M^3 + 18M^2 \right) R \\ & + \left[ \frac{27}{2} \left( -\frac{3\sqrt{3}}{32} + \frac{3}{8} \right) M^4 + \left( -\frac{9\sqrt{3}}{2} - \frac{4\sqrt{3}}{\pi} \right) M^3 + 6M^2 \right] \end{aligned} \quad (16)$$

#### 4.2. Characteristic Analysis

The Macro HDF is a random function of the random variable  $R$ . When  $R$  is 0.5 the macro HDF  $F(M)$  reaches the minimum value that is consistent with the traditional SVPWM scheme[2], which is expressed as Equation (17).

$$F_{\min}(M) = \frac{9}{8} \left( \frac{3}{2} - \frac{9\sqrt{3}}{8\pi} \right) M^4 - \frac{4\sqrt{3}}{\pi} M^3 + \frac{3}{2} M^2 \quad (17)$$

When  $R$  is 0 or 1, the macro HDF  $F(M)$  reaches the maximum value, and the corresponding value is expressed as

$$F_{\text{Max}}(M) = \frac{81}{16} \left( 1 - \frac{1}{4} \frac{\sqrt{3}}{\pi} \right) M^4 - \left( \frac{9}{2} + \frac{4}{\pi} \right) \sqrt{3} M^3 + 6M^2 \quad (18)$$

As to the typical discontinuous SVPWM schemes DPWMMIN, DPWMM, DPWM0, DPWM1, DPWM2, and DPWM3 discussed in [2], the DPWM3 has the minimum macro HDF that is expressed as

$$F_{\text{DPWM3}}(M) = \frac{27}{8} \left( 1 + \frac{1}{2} \frac{\sqrt{3}}{\pi} \right) M^4 + \left( \frac{45}{2\pi} - \frac{31\sqrt{3}}{\pi} \right) M^3 + 6M^2 \quad (19)$$

The difference between Equations (18) and (19) is

$$\begin{aligned} \Delta F &= F_{\text{DPWM3}}(M) - F_{\text{Max}}(M) \\ &= \frac{27}{16} \left( \sqrt{3} + \frac{3}{4} \frac{\sqrt{3}}{\pi} - 1 \right) M^4 + 9 \left( \frac{\sqrt{3}}{2} - \frac{3\sqrt{3}}{\pi} + \frac{5}{2\pi} \right) M^3 > 0 \end{aligned} \quad (20)$$

This shows that the proposed new RZDSVPWM scheme has more excellent harmonic performance than the 6 typical discontinuous schemes discussed in [2] in the respect of harmonic distortion.

If the expected value (or mathematical expectation, or mean) of  $R^2$  and  $R$  are expressed as  $E(R^2)$  and  $E(R)$ , respectively, the mean value of the macro HDF can be computed using Equation (21).

$$\begin{aligned} F_{\text{Mean}}(M) &= \left( \frac{27}{2} M^4 - 18\sqrt{3} M^3 + 18M^2 \right) E(R^2) - \left( \frac{27}{2} M^4 - 18\sqrt{3} M^3 + 18M^2 \right) E(R) \\ &\quad + \left[ \frac{27}{2} \left( -\frac{3\sqrt{3}}{32} + \frac{3}{8} \right) M^4 + \left( -\frac{9\sqrt{3}}{2} - \frac{4\sqrt{3}}{\pi} \right) M^3 + 6M^2 \right] \end{aligned} \quad (21)$$

If the random variable  $R$  obeys a uniform distribution in the interval  $[0, 1]$ ,  $E(R^2)$  is  $1/3$  and  $E(R)$  is  $0.5$ . The maximum, minimum and mean values of the macro HDF can be computed using the Equations (17), (18) and (21), as shown in Figure 4.

Since the uniform distribution is very simple, it is very easy to compute the mean value and the standard deviation. The closed-form expressions for the mean values  $E(R^2)$  and  $E(R)$  are not always possible or simple if the probability distribution law of the random variable  $R$  is very complex. Therefore, the numerical method is preferable.

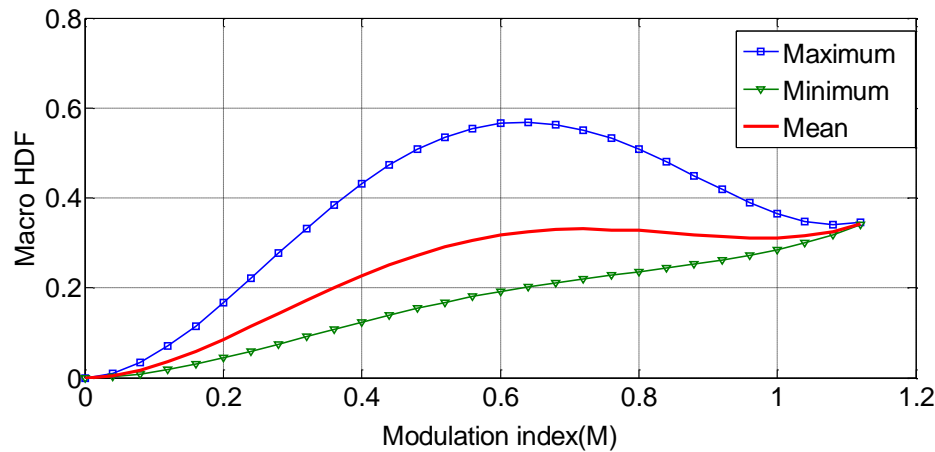


**Figure 4. Maximum, Minimum and Mean Values of the Macro Harmonic Distortion Factor(HDF)**

The Monte Carlo method is most effective in handling the random sampling simulation problem, making it by far the most widely-used method. By regarding the concerned random variables as pseudorandom numbers, the sampling pseudorandom numbers can be generated using the pseudorandom generating algorithm. The values of the random function, for example  $R^2$ , are then computed at each pseudorandom sampling number. The numerical character of the random function, for example  $R^2$ , is finally computed.

The theoretical mean value and standard deviation of the random function  $R^2$  can be computed as

$$\left\{ \begin{aligned} E(R^2) &= \int_0^1 R^2 dR = \frac{1}{3} \approx 0.3333333333333333 \\ \sigma(R^2) &= \sqrt{\int_0^1 (R^2 - E(R^2))^2 dR} = \sqrt{\int_0^1 \left(R^2 - \frac{1}{3}\right)^2 dR} = \frac{2\sqrt{5}}{15} \approx 0.298142396999972 \end{aligned} \right. \quad (22)$$

MATLAB provides many functions to generate pseudorandom numbers that obey the specified distributions. For example, rand returns a matrix containing pseudorandom values drawn from the standard uniform distribution in the open interval(0,1), and randn generates values from the standard normal distribution. To compute the mean value and the standard deviation of  $R^2$  is very simple and convenient in the Matlab environment, and the codes are as follows for that the random variable R obeys a uniform distribution in the interval (0, 1). The computation result is shown in Table 1 for three running times.

```
N=100000;myRandVariable=rand(1,N);
myRandFunction=myRandVariable.*myRandVariable;
myMean=mean(myRandFunction);myStd=std(myRandFunction)
```

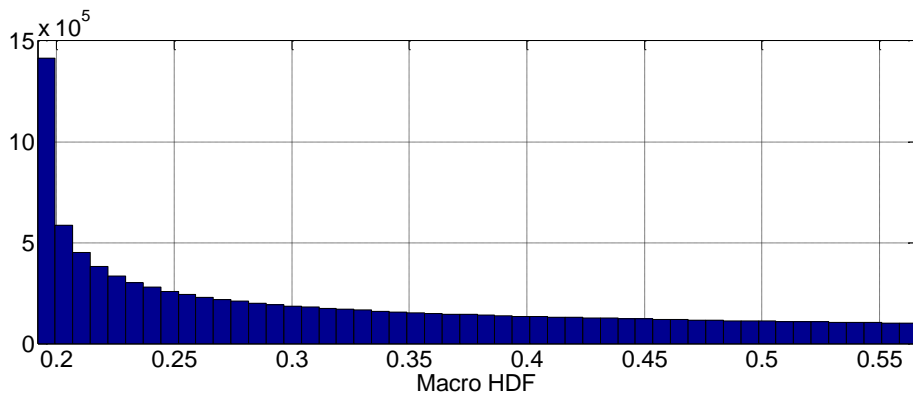


**Table 1. Mean Value and Standard Deviation Using Monte Carlo Method**

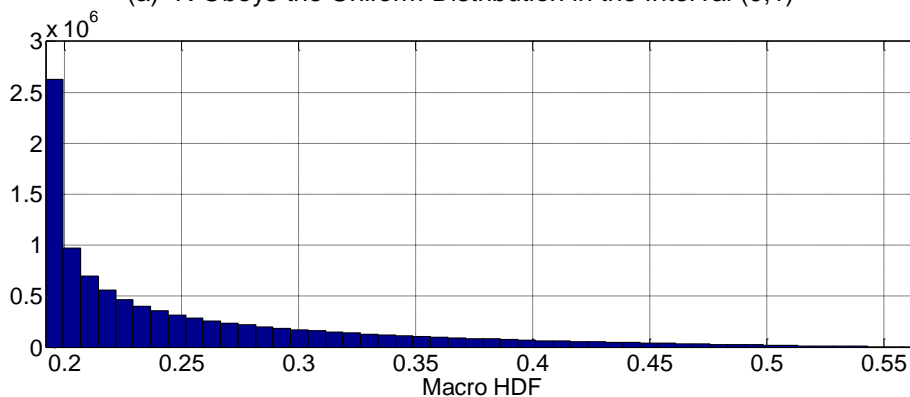
No.	1	2	3
Mean value	0.3351106777453	0.3345565272980	0.3341411457469
Standard deviation	0.2988918603275	0.2986761953746	0.2984279266023

It can be found that there are errors between the values in theory computation and the Monte Carlo method. It should be pointed out that the sampling number, the variable N in the above Matlab codes, has significant influence on the computation errors. The sampling number should be large enough if a high computation precision is required. The distribution of the HDF can also be computed using the Monte Carlo method. The frequency histograms (or the distributions) of the macro HDF are shown in Figure 5 for that the modulation index is 0.6 and the sampling number is 10000000. Figure 5(a) shows the distribution if R obeys the uniform distribution in the interval (0,1), while Figure 5(b) shows the distribution if R obeys the symmetrical triangle distribution in the interval (0,1). The probability density function of the symmetrical triangle distribution is expressed as

$$f(R) = \begin{cases} 4R & 0 < R \leq 0.5 \\ 2 - 4(R - 0.5) & 0.5 < R \leq 1 \end{cases} \quad (23)$$



(a) R Obeys the Uniform Distribution in the Interval (0,1)



(b) R Obeys the Symmetrical Triangle Distribution in the Interval (0,1)

**Figure 5. The Macro HDF Distributions of the New RZDSVPWM Scheme for That The Modulation Index is 0.6 and the Sampling Number is 10000000**

From the concerned theorem in probability theory and mathematical statistics, it is well known that the sum of two independent and identical random variables obeys the

symmetrical triangle distribution. The pseudorandom values drawn from the triangle distribution in MATLAB can be generated using the uniform distribution generation function rand. The codes are as follows.

```
N=10000000;M=60;myRand1=rand(N,1);myRand2=rand(N,1);
myRand3=(myRand1+myRand2)/2;hist(myRand1,M);h= findobj(gca,'Type','patch');
set(h,'FaceColor','b','EdgeColor','w');figure;hist(myRand3,M);
h = findobj(gca,'Type','patch');set(h,'FaceColor','b','EdgeColor','w')
```

The function of the codes is to generate two series of random numbers (that represent the two random variables obeying the uniform distribution), compute the summation series of the two series(that represent the random variable obeying the triangle distribution) and plot the frequency histograms. The running result is shown in Figure 6. Likewise, the random variables that obeys the other distribution can also be gotten from the standard uniform distribution random variable.

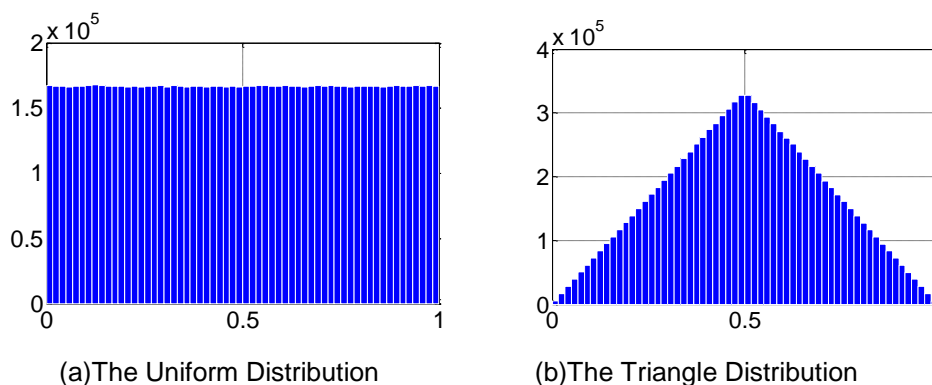
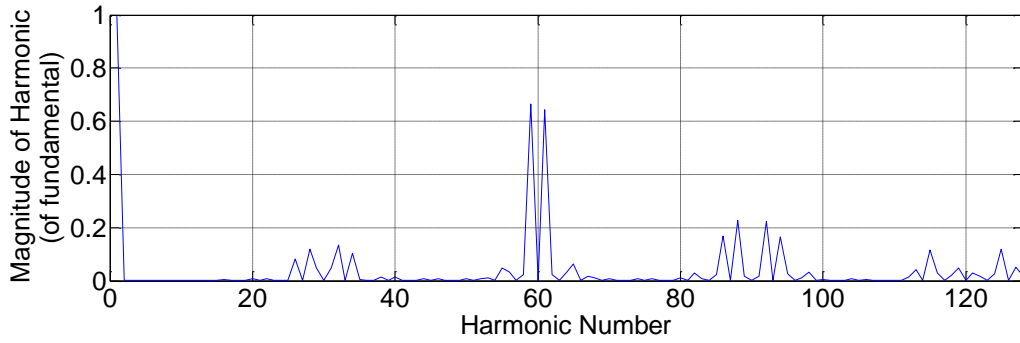


**Figure 6. The Frequency Histograms Generated using the Monte Carlo Method for That the Sampling Number is 10000000**

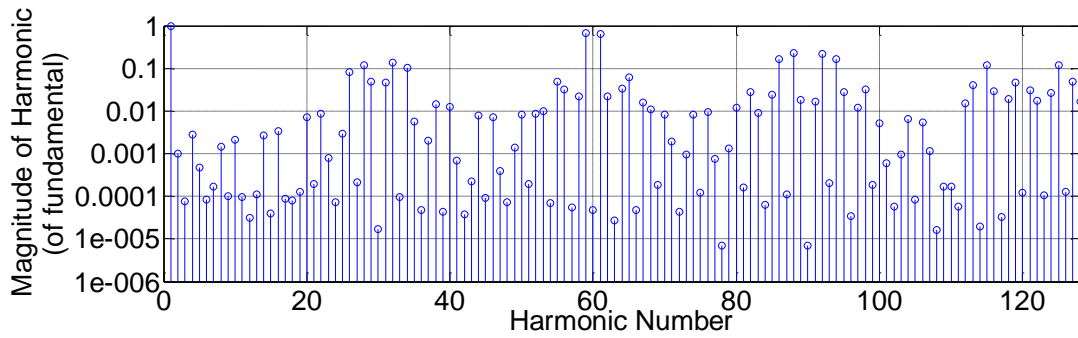
## 5. Simulation and Spectrum Analysis

A model was built in the engineering software package to analyze and demonstrate the characteristic of the new RZDSVPWM scheme. For the commonly used symmetrical 7-segment SVPWM scheme, the partitioning ratio of the two zero vectors is 0.5. For example, the DC bus voltage is 100V, the fundamental wave frequency is 60Hz and the switching frequency is 1800Hz. The harmonic spectrum of the line voltage between Phase A and Phase B is shown in Figure 7 given that the modulation index is 0.7. For the RZDSVPWM scheme, the duration time distribution ratio of the two zero-vectors described in Equation (7) is random. If the random variable  $R$  obeys a uniform distribution in the interval  $[0, 1]$ , the computation result is shown in Figure 8.

The remarkable harmonic spectrum difference between the deterministic SVPWM scheme and the proposed RZDSVPWM scheme can be found and compared easily. The random SVPWM scheme can significantly suppress the cluster harmonic magnitudes around the integer multiple switching frequency. The peak magnitude around the 60th harmonic is more than 60% of that of the fundamental in the deterministic SVPWM scheme shown in Figure 7, while it is only about 40% for the RZDSVPWM scheme shown in Figure 8. The proposed scheme of random zero vector partitioning has better effect on reducing the cluster harmonic magnitudes.

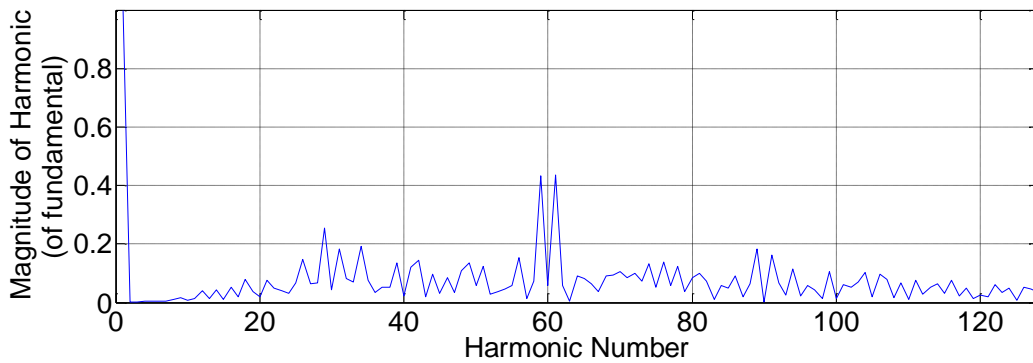


(a) Harmonic Spectra of the Line Voltage between Phase A and B Plotted using the Linear Scale for both Axes

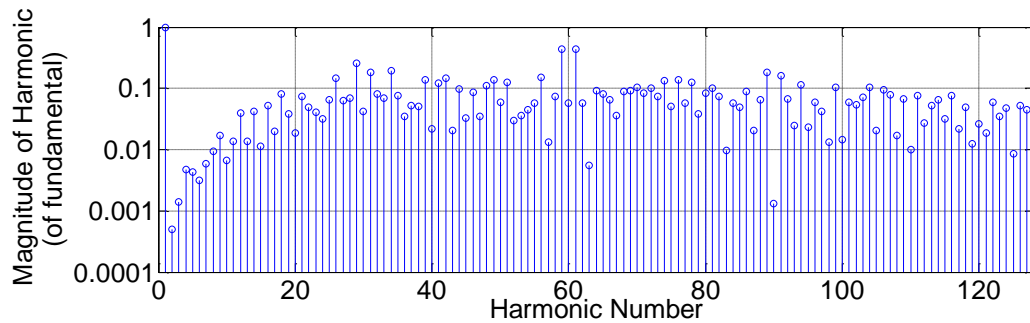


(b) Harmonic Spectra of the Line Voltage between Phase A and B Plotted using a Base 10 Logarithmic Scale for the Magnitude-axis and a Linear Scale for the Harmonic Number-axis

**Figure 7. The Computation Result for The Deterministic Symmetrical 7-Segment SVPWM Scheme**



(a) Harmonic Spectra of the Line Voltage between Phase A and B Plotted using the linear Scale for Both Axes



(b) Harmonic Spectra of the Line Voltage between Phase A and B Plotted using a Base 10 Logarithmic Scale for the Magnitude-axis and a Linear Scale for the Harmonic Number-axis

**Figure 8. The Computation Result for the Proposed RZDSPWM Scheme**

## 6. Conclusion

A new RZDSPWM scheme with a fixed randomization range is proposed. The implicit modulating voltages, the derivation procedure of the micro and macro HDF are given in detail. The analysis and computation results show that the proposed randomization scheme has several advantages. Firstly, the range of the randomization duration time of the zero vectors is fixed, and the fixed range is a linear function of the modulation index and the function expression is very compact and simple, which makes the scheme easily implemented in the digital control system. In addition, if the distribution law of the random variable is symmetrical with respect to 0.5, the mean of the random part in the implicit modulating voltage wave is zero. The standard deviation can be made constant if the distribution of the random variable in all switching period is identical. The random part of the implicit modulating voltage wave can be regarded as stationary random process, so it can be conveniently analyzed using the corresponding tool and theory. Finally, the proposed scheme has excellent performance on suppressing the cluster harmonic magnitudes around the integer multiple switching frequency. If the scheme is combined with other random schemes, more excellent performance can be gotten. However, it should be noticed that the spectrum of the inverter output waveform depends not only on the harmonic in the modulation voltage wave, but also on the PWM strategy, and the theoretical expression is very complicated. To get the theoretical expression is our future work.

## Acknowledgments

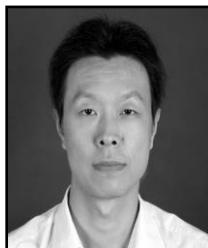
This work is supported by National Science Foundation of China (No. U1304525). The author would like to thank the anonymous reviewers for their valuable work.

## References

- [1] X. Mao, J. A. Kumar and A. Rajapandian, "Hybrid Interleaved Space Vector PWM for Ripple Reduction in Modular Converters", *IEEE Transactions on Power Electronics*, vol. 26, no. 7, (2011), pp. 1954-1967.
- [2] D. G. Holmes and T. A. Lipo, "Pulse Width Modulation for Power Converters: Principles and Practice", IEEE Press, USA, (2003).
- [3] B. K. Bose, "Modern Power Electronics and AC Drives", Prentice Hall, UK, (2001).
- [4] G. Chen, "PWM Inverter Technology and Application", China Electric Power Press, Beijing China, (2007).
- [5] P. N. Reddy, J. Amarnath and P. L. Reddy, "Hybrid Random PWM Algorithm for Direct Torque Controlled Induction Motor Drive for Reduced Harmonic Distortion", *Proceedings of 2011 Annual IEEE India Conference: Engineering Sustainable Solution*, New York, USA, (2011) December 16-18.

- [6] S. Kaboli, J. Mahdavi and A. Agah, "Application of Random PWM Technique for Reducing the Conducted Electromagnetic Emissions in Active Filters", *IEEE Transactions on Industrial Electronics*, vol. 54, no. 4, (2007), pp. 2333-2343.
- [7] S. H. Na, Y. G. Jung, Y. C. Lim and S. H. Yang, "Reduction of Audible Switching Noise in Induction Motor Drives Using Random Position Space Vector PWM", *IEEE Proceedings Electric Power Applications*, vol. 149, no. 3, (2002), pp.195-200.
- [8] M. Zigliotto and A.M. Trzynadlowski, "Effective Random Space Vector Modulation for EMI Reduction in Low-cost PWM Inverters", *Proceedings of the 7th International Conference on Power Electronics and Variable Speed Drives*, New York, USA, (1998) September 21-23.
- [9] N. Boudjerda, A. Boudouda, M. Melit, B. Nekhoul, K. EI Khamlichi Drissi and K. Kerroum, "Optimized Dual Randomized PWM Technique for Reducing Conducted EMI in DC-AC Converters", *Proceedings of the 10th International Symposium on Electromagnetic Compatibility*, New York, USA, (2011), September 26-30.
- [10] D. Jiang and F. F. Wang, "Variable Switching Frequency PWM for Three-Phase Converters Based on Current Ripple Prediction", *IEEE Transactions on Power Electronics*, vol. 28, no. 11, (2013), pp. 4951-4961.
- [11] G. Chen, Z.Wu and Y. Zhu, "Harmonic Analysis of Random Pulse Position Space Vector PWM", *Journal of Tongji University*, vol. 40, no. 7, (2012), pp.1111-1117.
- [12] Z. Wu, Guoqiang Chen, Y. Zhu and G. Tian, "Harmonic Analysis of Random Zero-vector Distribution Space Vector Pulse Width Modulation", *Journal of Tongji University*, vol. 39, no. 6, (2011), pp. 901-907.
- [13] G. Chen, M. Zhang and J. Zhao, "Harmonic Distortion Factor of A Hybrid Space Vector PWM Based on Random Zero-vector Distribution and Random Pulse Position", *Advances in Information Sciences and Service Sciences*, vol. 4, no.16, (2012), pp. 242-250.
- [14] Y. Lu, X. Huang, B. Zhang and Z. Mao, "Two Chaos-Based PWM Strategies for Suppression of Harmonics", *Proceedings of the 6th World Congress on Intelligent Control and Automation*, Dalian, China, (2006) June 21-23.
- [15] G. Chen and J. Kang, "A Randomization Method to Zero Vector Distribution of Space Vector Pulse Width Modulation", *Advanced Science and Technology Letters*, vol. 123, (2016), pp. 167-107.

## Authors



**Guoqiang Chen** is currently an associate professor in the School of Mechanical and Power Engineering, Henan Polytechnic University, China. His research interests include robot technology, electric vehicle control, motor control, pulse width modulation technology and software design.

